Isospin splitting of the giant dipole resonance in ^{89}Y

E. Van Camp, D. Ryckbosch, R. Van de Vyver, E. Kerkhove, P. Van Otten, and P. Berkvens

Laboratorium voor Kernfysica, Rijksuniversiteit Gent, B-9000 Ghent, Belgium

(Received 6 April 1984)

The total cross section for the reaction ^{89}Y$(\gamma,p)^{88}$Sr has been measured; the existence of the coherent $T_>$ state is clearly demonstrated. Using our (γ,p) and the available (γ,n) results, a strength ratio of the $T_>$ to $T_<$ component $S_>/S_<$ equal to 0.13—0.14 is obtained. By determining the cross sections for various proton decay channels, the escape $\Gamma^\uparrow$ and spreading $\Gamma^\downarrow$ widths for the $T_>$ resonance were deduced. The direct decay probability of the $T_>$ state has been found to be $\Gamma^\uparrow/\Gamma = 0.17\pm0.03$.

I. INTRODUCTION

Because of the isovector character of the electric dipole operator, both $T_< = T$ and $T_> = T+1$ states can be excited by $E1$ photon absorption on a non-self-conjugate nucleus (with ground state isospin T). For many years it has generally been accepted that nearly the entire electric dipole strength in the giant dipole resonance (GDR) region of such nuclei is shared among coherent states that possess either a $T_<$ or $T_>$ isospin quantum number.[1-3] The theoretical estimates of the strength ratio and energy separation of both $T_<$ and $T_>$ dipole states, as given by[4,5]

$$\frac{S_>}{S_<} = \frac{1}{T}\frac{1-\frac{3}{2}TA^{-2/3}}{1+\frac{3}{2}A^{-2/3}} , \tag{1}$$

$$E_> - E_< = 60\frac{T+1}{A} \text{ MeV} , \tag{2}$$

with

$$S = \int \frac{\sigma(E)}{E}dE ,$$

seem to adequately describe the experimental data. Although the energy location of the coherent $T_>$ state is well determined over a wide mass region mainly by means of (p,γ_0) reactions,[1,6] the total $T_>$ strength is less well known experimentally since it requires the knowledge of both total (γ,n) and (γ,p) or the total photoabsorption cross sections. On the other hand, an additional difficulty arises in nonspherical nuclei, where deformation splitting of the GDR may obscure the $T_>$ assignment of the observed structure. Consequently, the $T_>$ strength determination is most reliable in spherical nuclei.

The simple features of the dipole resonance in the quasispherical nucleus ^{89}Y (with $T=\frac{11}{2}$) may make a distinct observation of the $T_>$ strength possible. Basically, one coherent state underlies the $T_<$ GDR of this nucleus[7,8] such that the line shape of the $T_<$ cross section can be described by a single Lorentzian. This single Lorentz line behavior is most clearly observed in the (γ,n) experiments of Berman *et al.*[9] and of Leprêtre *et al.*,[10] and in the photon scattering experiment of Arenhövel and

Maison;[8] this knowledge is essential for the quantitative determination of the total $T_>$ strength from the present measurement.

Experimentally, total $T_>$ strengths in ^{89}Y have been estimated previously by means of (γ,γ') and $(e,e'p)$ reactions,[8,11] which seem to be in agreement with the prediction of expression (1). However, both results show a broad $T_>$ resonance in contrast with a $T_>$ strength distribution consisting of several distinct peaks with a rather narrow width, as was deduced from (p,γ_0) measurements in the $A=90$ mass region.[1,12-14] Theoretically, the $T_>$ strength distribution in ^{89}Y has been calculated within a shell model framework[7,15] since its ground state has a very simple configuration consisting of a closed $N=50$ neutron shell and one proton in the $2p_{1/2}$ subshell.

The present work aims at the study of the $T_>$ giant dipole resonance in ^{89}Y by means of the ^{89}Y$(\gamma,p)^{88}$Sr reaction. It is our intention not only to conclusively prove the existence—and to estimate the strength—of the coherent $T_>$ electric dipole state, but we also hope to shed some light on the decay properties of this state.

II. EXPERIMENTAL PROCEDURE

A natural ^{89}Y foil with a thickness of 13.3 mg/cm^2 was irradiated with a bremsstrahlung photon beam from an electron linear accelerator. Photoprotons were detected at seven angles simultaneously, ranging from 37° to 143°, by means of uncooled 3 mm thick Si(Li) detectors. Further details about the experimental arrangement can be found in Ref. 16. Photoproton energy spectra were measured at bremsstrahlung end point energies between 14 and 25 MeV, going up in 1 MeV steps.

Our technique of artificially constructing a pseudomonoenergetic photon spectrum by means of an algebraic sum of three suitably normalized bremsstrahlung spectra with consecutive end point energies (as described in Ref. 17) enables us to determine the integrated-over-angles (γ,p) cross sections for reaction processes leading to various states (or groups of states) in the residual nucleus ^{88}Sr. Obviously the energy resolution of the obtained results cannot be better than about 1 MeV. However, since the first excited state in ^{88}Sr is located at 1.84 MeV the ground state cross section $\sigma(\gamma,p_0)$ can be direct-
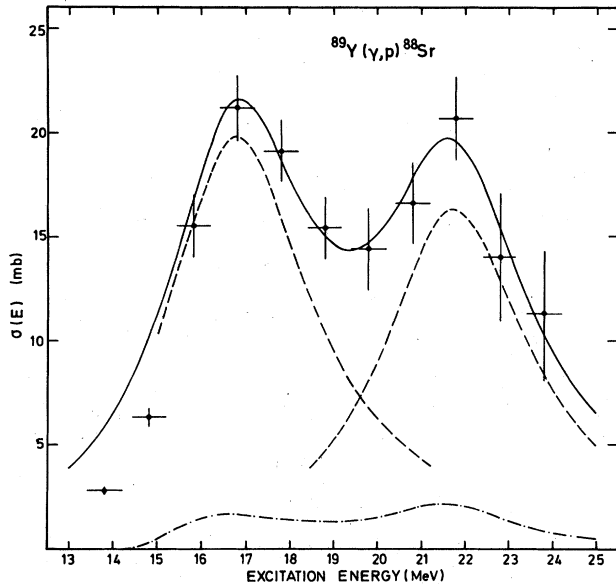
FIG. 1. The data points show the experimentally determined total $^{89}Y(\gamma,p)^{88}$Sr cross section, while the full line represents the sum of the two Lorentzians (shown as dashed lines) that were fitted to the $T_<$ and $T_>$ coherent dipole states, respectively (the parameters are listed in Table I). The dotted-dashed line is the result of a statistical calculation using a Hauser-Feshbach formalism, representing the contribution to the statistical cross section of low-energy photoprotons ($T_p < 4$ MeV) that are lost in the background region.

ly deduced, with a better energy resolution ($\simeq 0.4$ MeV) from the experimental data.[16] Due to the fact that in each measured photoproton spectrum the background[17] extends to a proton kinetic energy $T_p \simeq 4$ MeV, only protons could be observed with a kinetic energy larger than this energy. Consequently the artificially-generated proton spectrum contains no protons with an energy lower than 4 MeV.

The integrated-over-angles total (γ,p) cross section, depicted in Fig. 1, was then determined from the integral over the proton energy of the artificially-generated photoproton spectra. As is indicated by a Hauser-Feshbach statistical calculation, the result of which is also shown in Fig. 1, only a small fraction of photoprotons lost in the background region contributes to the cross section in the 14—25 MeV energy region. As such, our derived (γ,p) cross section should approximate the total photoproton cross section very well.

III. DISCUSSION OF RESULTS

The ^{89}Y giant dipole resonance is located[8-10] at $E_< = 16.8$ MeV, and as a consequence of relation (2), the $T_>$ resonance should be expected around $E_> \simeq 21$ MeV. The decay scheme of this GDR is shown in Fig. 2 for both the proton and the neutron channel. The isospin selection rules are indicated by the squared isospin vector coupling coefficients. If isospin is a conserved quantum

number, neutron decay from the $T_>$ state to residual $T - \frac{1}{2}$ states is forbidden while, on the other hand, the allowed n decay to $T + \frac{1}{2}$ states will be very much suppressed by barrier effects as the high Coulomb displacement energy ΔE_C ($\simeq 12.4$ MeV) locates the lowest $T + \frac{1}{2}$ isobaric analog state in ^{88}Y at an energy of about 8 MeV, which corresponds to a neutron separation energy of 19.5 MeV in ^{89}Y. Consequently, this selection rule together with the strong hindrance of $T_<$ proton emission due to the Coulomb barrier, will make the (γ,p) reaction a favorable tool for the possible detection of the $T_>$ resonance in ^{89}Y. However, a distinct peak observed in the photoproton cross section can only be thought of as originating from the coherent $T_>$ state if both the derived strength and the energy location are consistent with relations (1) and (2), respectively, and if simultaneously the isospin selection rule holds, i.e., if the observed resonance is relatively much more important in the (γ,p) than in the (γ,n) channel.

A. The total (γ,p) cross section

From Fig. 1 it is observed that two clearly separated resonances with comparable strength are presented in the total (γ,p) cross section. The lower component at $E = 16.8$ MeV coincides with the $T_<$ GDR detected in (γ,n) experiments (see Table I), while the other resonance is located at 21.8 MeV, which is about the energy where the $T_>$ state can be expected. For comparison the (γ,n) cross sections of Leprêtre et al.[10] and of Berman et al.[9] are shown in Fig. 3.

A single Lorentz line

$$\sigma(E) = \sigma_0 \frac{(E\Gamma)^2}{(E^2 - E_R^2)^2 + (E\Gamma)^2} \qquad (3)$$

fits the lower energy part of these (γ,n) cross sections very well, in contrast with the energy region above 19 MeV, where a neutron excess above this line is clearly present. Apparently this neutron excess coincides with the second maximum around 21.8 MeV in the (γ,p) channel. It is striking that, if this excess cross section is attributed to a $T_>$ character, it only represents a minor fraction of the total neutron cross section as clearly distinct from the situation in the (γ,p) channel. Such behavior, as suggested by the isospin selection rules, stresses the identification of the second maximum in the (γ,p) cross section as being the $T_>$ state; note that the influence of the $\Delta T = 1$ quadrupole resonance on the cross section near 22 MeV can be neglected because in ^{89}Y it is located at 28 MeV and possesses a much larger width,[18] i.e., 7—10 MeV.

Although Lorentz lines (3) may not necessarily describe the correct shape of the cross section components in the (γ,p) channel, for convenience we have fitted a sum of two Lorentzians to the total (γ,p) cross section. In this fit, the width ($\Gamma_< = 4$ MeV) and energy location ($E_< = 16.8$ MeV) of the lower resonance were fixed by the (γ,n) experimental data. The result is shown in Fig. 1, while the derived parameters are presented in Table I.
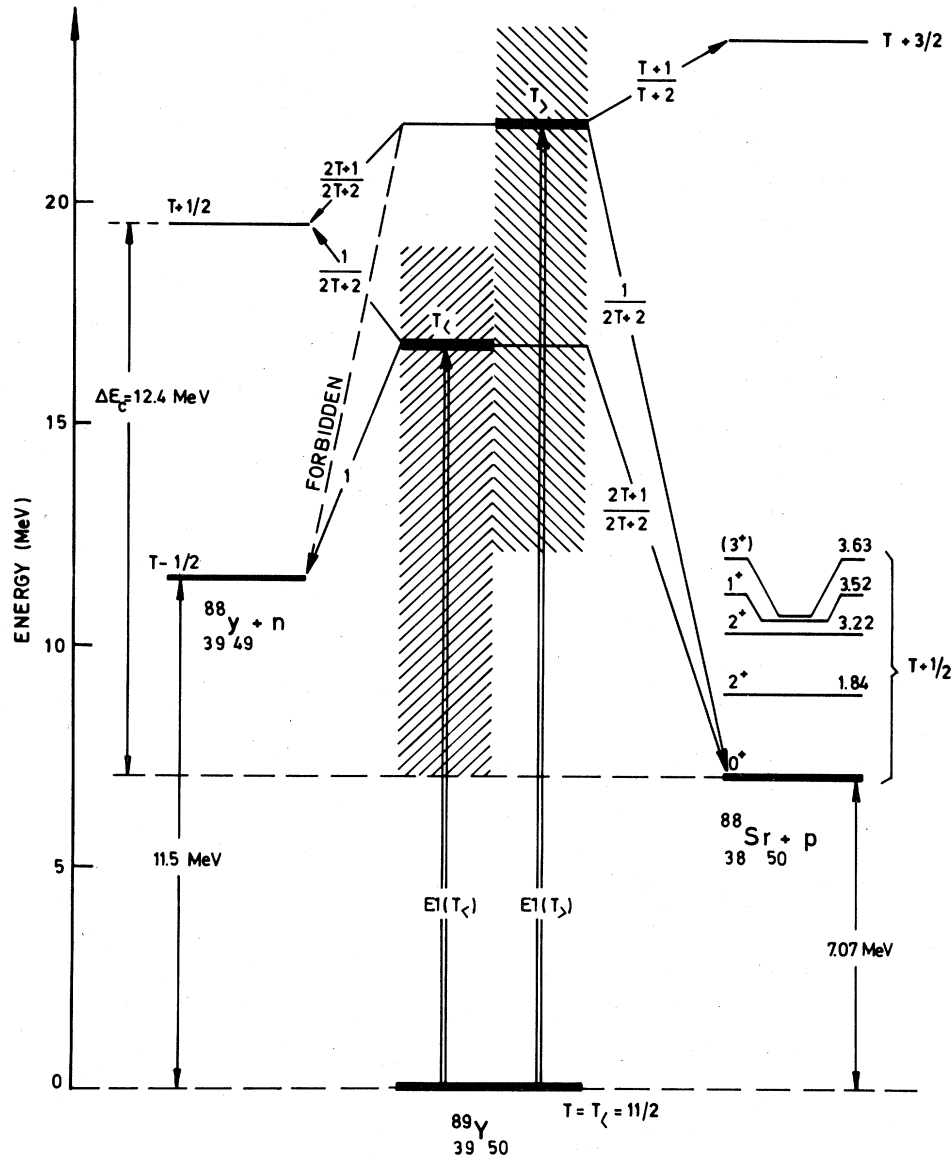
FIG. 2. The decay scheme of the $T_<$ and $T_>$ giant dipole resonances in ^{89}Y.

As such, the strength

$$S = \int \frac{\sigma(E)}{E} dE \simeq \frac{\pi}{2} \frac{\sigma_0 \Gamma}{E_R}$$

of the $T_<$ and $T_>$ resonances in the proton channel can be determined in a straightforward way. However, in order to deduce the total $T_>$ strength it is essential to know what fraction of the (γ,n) cross section is due to the decay of the $T_>$ state. For this purpose it is assumed that the single Lorentz line correctly describes the shape of the $T_<$ resonance, even in the energy region around 21 MeV. This assumption is plausible since, as was pointed out before, basically one $T_<$ dipole state is underlying the GDR.[7,8]

Unfortunately there is no agreement as far as the magnitude of the excess neutron cross section is concerned be-

tween the results of Livermore[9] and of Saclay.[10] However, the existence of this excess is beyond doubt and in an attempt to derive a meaningful result, a Lorentz line with the same $T_>$ parameters (energy and width) as deduced from our (γ,p) experiment was fitted to this neutron excess. The result is also depicted in Fig. 3 by the dashed lines, while the peak cross section values σ_0 are given in Table I.

Due to the fact that the separation energy for the (γ,np) reaction equals about 18.2 MeV, no substantial neutron-proton emission will occur below 22.5 MeV and, consequently, by summing the (γ,p) and the (γ,n) results nearly no double counting of the same decay process will be present. Using the estimated cross sections (Table I) for proton and neutron decay from the $T_>$ state, one arrives at a strength ratio $S_> /S_< = 0.14 \pm 0.02$ or 0.13 ± 0.02

TABLE I. Lorentz-line parameters for the $T_<$ and $T_>$ giant dipole resonances in ^{89}Y.

Experiment	$T_<$ Resonance energy E_R (MeV)	$T_<$ Peak cross section σ_0 (mb)	$T_<$ Width Γ (MeV)	$T_>$ Resonance energy E_R (MeV)	$T_>$ Peak cross section σ_0 (mb)	$T_>$ Width Γ (MeV)
(γ,n): Berman et al. (Ref. 9)	16.79±0.04	185 ±5	3.95±0.06		18 ±2[a]	
(γ,n): Leprêtre et al. (Ref. 10)	16.7 ±0.05	225 ±10	4.1 ±0.1		23 ±2[a]	
(γ,γ'): Arenhövel and Maison (Ref. 8)	16.4	210	3.95	21.5±0.2	22 ±2	4±0.3
(γ,p): Shoda et al. (Ref. 11)	(16.7)	17.3		(21.6)	17.3	
(γ,p): This experiment	16.8 ±0.3	19.8±1.5 20.8±1.5[b]	4.0 ±0.3	21.8±0.3	16.3±1.5 18.3±1.5[b]	4±0.5

[a]Estimated in the present analysis by fitting a Lorentz line to the excess neutron cross section.
[b]Estimated (γ,p) cross section taking into account the low-energy photoprotons lost in the background.

depending on whether the results of Berman et al.[9] or of Leprêtre et al.,[10] respectively, have been used. This value has to be compared to $S_>/S_< = 0.10$ as determined by relation (1). These various strength ratios are summarized
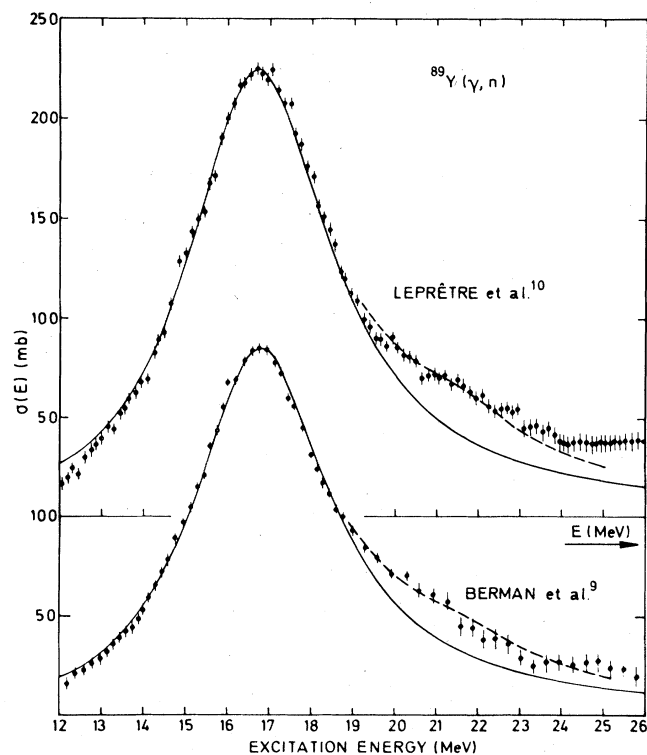

FIG. 3. The data points represent the experimentally determined ^{89}Y(γ,xn) cross section as determined by Leprêtre et al. (Ref. 10) and by Berman et al. (Ref. 9). The full line shows a fit of one Lorentzian to the main peak ($T_<$) in the cross section, while the dashed line is the result of a fit of a second Lorentz line ($T_>$) to the excess neutron cross section, using the same $T_>$ parameters (energy and width) as deduced from Fig. 1 (see also Table I).

in Table II. At this point it may be concluded that the second maximum in the total photoproton cross section actually represents the $T_>$ collective dipole state and that both the (γ,p) and (γ,n) $T_>$ strengths can be deduced with reasonable accuracy.

Our total (γ,p) cross section is comparable in magnitude with the results obtained in an (e,e'p) experiment performed at 90° by Shoda et al.[11] This 90° differential cross section was converted to a total (γ,p) cross section (shown in Fig. 4) using the angular distribution for the same reaction in ^{90}Zr. Although reasonably good agreement with the present data is observed, at the high-energy side the (e,e'p) cross section seems to reach a constant value; con-
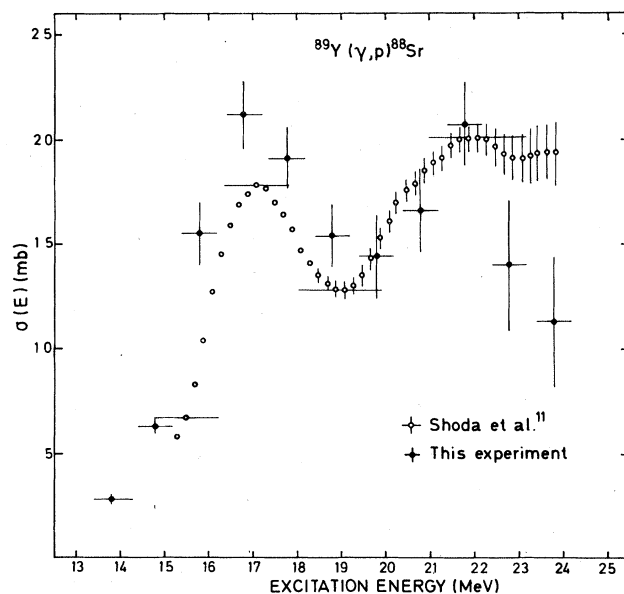

FIG. 4. Comparison of our total ^{89}Y(γ,p) cross section data (closed circles) with the results obtained in an (e,e'p) experiment by Shoda et al. (Ref. 11) (open circles).

TABLE II. The strength ratio $S_>/S_<$ for the $T_>$ to $T_<$ GDR in ^{89}Y.

Source	$S_>/S_<$	
Theory (Ref. 4)	0.10	
(γ,γ') (Ref. 8)	0.10	
(γ,p) (Ref. 11)	0.12[b]	
This experiment + (γ,n) (Ref. 10)	0.12±0.02	0.13±0.02[a]
+ (γ,n) (Ref. 9)	0.13±0.02	0.14±0.02[a]

[a]Using our data from Table I, taking into account the low-energy photoprotons lost in the background.
[b]Using the (γ,n) data from Ref. 10.

sequently, the width of the $T_>$ resonance could not be deduced from these data. The reason for this unexpected behavior should perhaps be sought in the yield curve unfolding technique used in the (e,e'p) analysis.

The energy location of the $T_>$ resonance as calculated by Vergados and Kuo[7] and by Hughes and Fallieros,[15] using a shell model approach, agrees fairly well with the present data. The latter calculation shows that (for each J) the one coherent $T_>$ state, obtained in a schematic model, is fragmented over many states—even nondoorway ones—due to the residual interaction. As such, the broad $T_>$ resonance observed in our (γ,p) experiment can be interpreted as being caused by a coherent $T_>$ doorway state that is spread over more complicated states which may be detected as intermediate structure in (p,γ_0) cross sections performed with better energy resolution.

B. Cross sections for the identified proton-hole channels

The residual nucleus ^{88}Sr has a simple structure and its excited states have extensively been studied both experi-

mentally[19] and theoretically.[20] By means of the ^{89}Y(d,^{3}He)^{88}Sr pickup reaction[19] only five proton-hole states (referring to the ^{89}Y ground state) have been identified, all located below 4 MeV; these are also depicted in Fig. 2. The other four known excited states in ^{88}Sr below 4 MeV have a more complicated structure, while above 4 MeV the level density and the complexity of the states in-
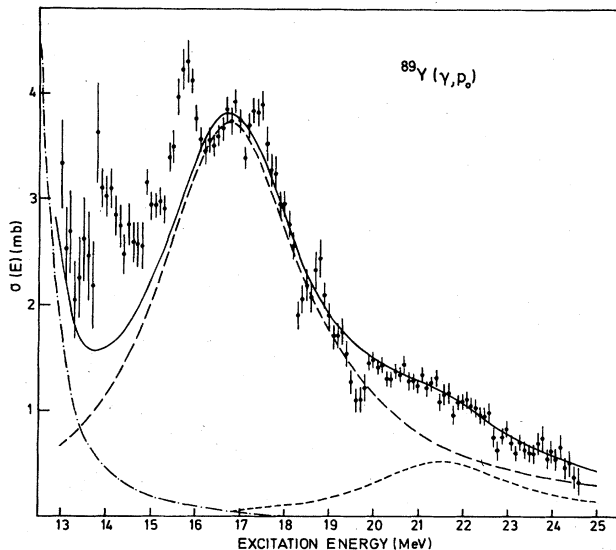

FIG. 5. The points with error bars show our experimentally determined total ^{89}Y(γ,p$_0$) cross section, while the dashed lines represent the fitted $T_<$ and $T_>$ Lorentzians using the parameters (E_R,Γ) listed in Table I. The dotted-dashed line is the result of a statistical (γ,p_0) calculation using a Hauser-Feshbach formalism. The full line shows the sum of those three components.
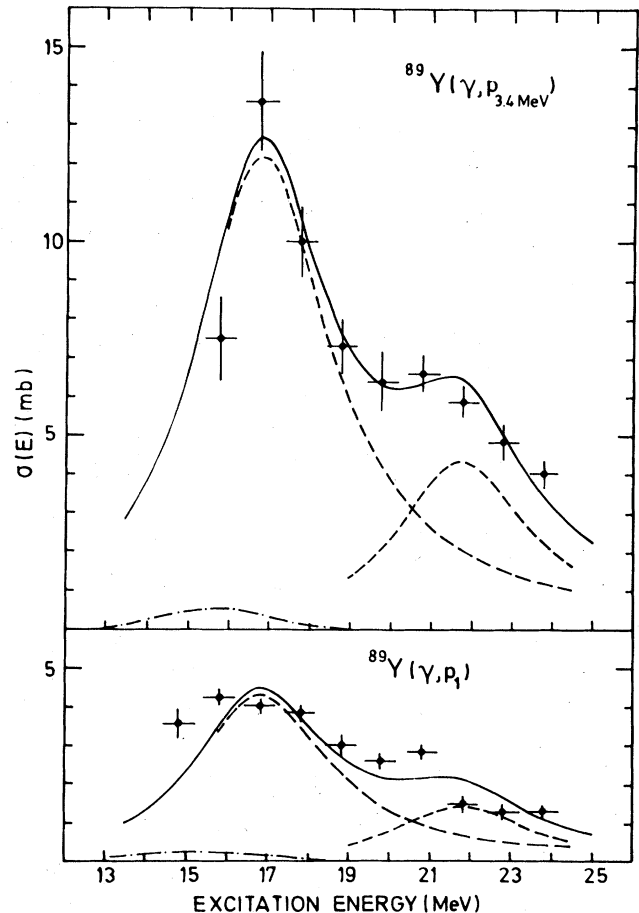

FIG. 6. The data points represent our experimentally determined ^{89}Y(γ,p$_1$) and (γ,p$_{3.4 \text{ MeV}}$) cross sections for the photoproton decay to the first excited state and to the group of excited states around 3.4 MeV in the residual nucleus ^{88}Sr. The dashed lines show the fitted $T_<$ and $T_>$ components using the parameters (E_R,Γ) from Table I. The dotted-dashed line is the result of a statistical (γ,p_1) and (γ,p$_{3.4 \text{ MeV}}$) calculation using a Hauser-Feshbach formalism. The full line depicts the sum of both Lorentzians.

creases. Direct decay of the coherent 1p-1h doorway states leads to the simple hole states in ^{88}Sr, while the nondirect decay leads to the more complicated residual states.

As the proton-hole states in ^{88}Sr are well separated in energy, it was possible to identify decay to these states in the photoproton spectra that correspond to a pseudomonoenergetic photon flux;[17] three proton-hole channels were separated, i.e., the ground and the first excited state channel and the one leading to the group of three states around 3.4 MeV. The corresponding cross sections[16,17] are shown in Figs. 5 and 6. These cross sections reach their maximum at an energy where the $T_<$ resonance is located. Their direct decay nature is stressed by a Hauser-Feshbach calculation which shows a negligible statistical decay contribution to these hole states (see Figs. 5 and 6).

In first order of the electromagnetic interaction H_γ and in the doorway state approximation, the transition amplitude for photonuclear reactions is given by[21]

$$\langle b \mid T \mid a \rangle = \langle \chi_i^{(-)} \mid H_\gamma \mid a \rangle + \langle \chi_i^{(-)} \mid V \mid D \rangle$$
$$\times \frac{1}{E - E_D - \Delta E + \frac{i}{2}(\Gamma^\uparrow + \Gamma^\downarrow)} \langle D \mid H_\gamma \mid a \rangle$$

$$(4)$$

when only one doorway state $\mid D \rangle$ is considered. The distorted state $\mid \chi_i^{(-)} \rangle$ in channel i leads to the plane wave $\mid b \rangle$ describing the final state of the residual nucleus and

the relative motion of the outgoing proton. The quantity V signifies the residual interaction, which couples the doorway state $\mid D \rangle$ with the continuum.

This residual state, contained in $\mid \chi_i^{(-)} \rangle$, can be either a simple proton-hole state or a complicated state. In the latter case the first matrix element in (4) which describes the direct knockout photonuclear reaction vanishes due to the doorway hypothesis, which states that no complicated states can be directly excited by means of the one-body operator H_γ. The transition amplitude then describes a complicated nondirect decay process. However, the resonance term dominates even for the proton-hole channels[22] so that, in first approximation, the direct knockout term can be neglected.

In general, the escape ($\Gamma^\uparrow$) and the spreading ($\Gamma^\downarrow$) widths, as well as the energy shift ΔE with respect to the unperturbed doorway, are energy dependent. For medium and heavy nuclei this energy dependence generates the strength function (constant width Γ and resonance energy E_R) of the dipole state:

$$S(E) \sim \frac{1}{E} \frac{1}{\left[\frac{E^2 - E_R^2}{2E}\right]^2 + \frac{\Gamma^2}{4}} .$$

This phenomenologically obtained strength distribution leads to the familiar Lorentz line shape (3) which describes the GDR.

Keeping this in mind, the differential cross section for channel i can be written as

$$\frac{d\sigma_i}{d\Omega}(E) = \frac{2\pi}{\hbar} \frac{1}{\phi} \sum \mid \langle \chi_i^{(-)} \mid V \mid D \rangle \mid^2 \frac{\left[E_R^2 - \frac{\Gamma^2}{4}\right]^{1/2}}{E} \frac{1}{\left[\frac{E^2 - E_R^2}{2E}\right]^2 + \frac{\Gamma^2}{4}} \mid \langle D \mid H_\gamma \mid a \rangle \mid^2 \rho_i(E) , \qquad (5)$$

wherein $\rho_i(E)$ and ϕ represent the final state density and the incoming photon flux, respectively. The summation symbol takes into account the averaging over the polarizations in the initial state and the summation over the final state polarizations.

Introducing the Lorentz-shaped total absorption cross section $\sigma(E)$, the angle-integrated cross section in channel i becomes:

$$\sigma_i(E) = 2\pi \sum_{Sl} \mid \langle Sl;JT \mid V \mid D \rangle \mid^2 \rho_i(E) \frac{\sigma(E)}{\Gamma} \langle T_i t_i; T_{3i} t_{3i} \mid T\ T_3 \rangle^2 , \qquad (6)$$

wherein the last factor (in between angular brackets) signifies the isospin vector coupling coefficient. The final state vector is now written in the channel spin (S) representation and is coupled to the angular momentum J and the isospin T of the dipole state.

For direct decay to a proton-hole state, the expression

$$\Gamma_i^\uparrow = 2\pi \sum_{Sl} \mid \langle Sl;JT \mid V \mid D \rangle \mid^2 \rho_i(E) \langle T_i t_i; T_{3i} t_{3i} \mid T\ T_3 \rangle^2$$

$$(7)$$

represents the escape width of the dipole state $\mid D \rangle$ for channel i.

In the case when two doorway states (the $T_<$ and the $T_>$ coherent dipole states) dominate the cross section, the

conservation of isospin prevents the coupling between these two primary doorways such that no interference between these two takes place in the integrated-over-angles cross section, which is then given by summing (6) over the two isospins.

Although the shape of the cross section (6) for the proton-hole channels is not exactly described by a Lorentzian, the fact that the total (γ,p) cross section can be successfully fitted by such lines inclines us to approxi-

TABLE III. The deduced peak values of the $T_<$ and $T_>$ resonances, identified in the ^{89}Y(γ,p_0), (γ,p_1), and $(\gamma,p_{3.4 \text{ MeV}})$ decay channels. $P(E)$ denotes the mean transmission coefficient, while R_i signifies the ratio of the coupling matrix elements.

Channel i	Separation energy Q_i (MeV)	Peak cross section $\sigma_{0i}(<)$ (mb)	Peak cross section $\sigma_{0i}(>)$ (mb)	$\left[\dfrac{S_>}{S_<}\right]_i$	$\left[\dfrac{P(E_>)}{P(E_<)}\right]_i$	R_i
γ,p_0	7.07	3.7±0.3	0.5±0.1	0.10±0.03	1.1	7.5±3
γ,p_1	8.91	4.3±0.2	1.4±0.15	0.25±0.04	1.45	12.8±4
$\gamma,p_{3.4 \text{ MeV}}$	10.5	12.2±0.4	4.4±0.3	0.28±0.04	2.0	10 ±3

mate all individual cross sections (Figs. 5 and 6) by the same Lorentz line shapes (3). The escape widths (7) are then forced to be energy independent and they can be determined using (6) from the following expression:

$$\Gamma_i^\uparrow = \frac{\sigma_{0i}}{\sigma_0}\Gamma , \qquad (8)$$

wherein σ_{0i} and σ_0 represent the peak values of the cross section in channel i and in the total dipole photoabsorption cross section, respectively. The various σ_{0i} values for the three measured direct decay channels were obtained explicitly by fitting a sum of two Lorentzians to the cross sections, but keeping the values for the energies and widths equal to those deduced in the fit to the total (γ,p) cross section. The parameters are presented in Table III while the fitted curves are shown in Figs. 5 and 6. It is immediately observed that the $T_>$ resonance also contains a direct decay component in the photoproton channel.

Except for the (γ,p_0) reaction, the derived strength ratios $(S_>/S_<)_i$ for the three direct channels (Table III) differ significantly from $S_>/S_<$ as given in Table II. Their relation can be obtained from (6)

$$(S_>/S_<)_i = \frac{1}{2T+1}\left[\frac{P(E_>)}{P(E_<)}\right]_i \frac{\sum_{Sl}V_i^2(T_>)}{\sum_{Sl}V_i^2(T_<)}$$

$$\times \left[\frac{E_>-Q_i}{E_<-Q_i}\right]^{1/2}\frac{\Gamma_<}{\Gamma_>}\left[\frac{S_>}{S_<}\right] ,$$

wherein the mean (averaged over the orbital angular momentum l) transmission factors $P(E)$ are lifted out of the coupling matrix elements. The quantity Q_i represents the separation energy for channel i. From this expression, the ratio

$$R_i = \sum_{Sl}V_i^2(T_>)/\sum_{Sl}V_i^2(T_<)$$

of the coupling matrix elements connecting the $T_>$ or $T_<$ dipole state with the proton continuum can be derived for the various channels (Table III). The results reflect a stronger coupling of the $T_>$ state with the proton continuum than is the case for the $T_<$ state.

Since isospin is conserved in a direct decay process, the

only allowed direct neutron decay of the $T_>$ state leads to the $T+\frac{1}{2}$ analog states in ^{88}Y that are located above 19.5 MeV excitation energy. As such, direct $T_>$ neutron decay will be negligible. On the other hand, the nonstatistical $T_<$ neutron decay width has recently been published[23] and, as nearly no preequilibrium decay in the GDR of ^{89}Y is to be expected,[24] this width represents the neutron escape width $\Gamma_n^\uparrow$. Now, since the total (Table I) and the direct decay (Table III) cross sections have been determined for both the $T_<$ and the $T_>$ resonances, the respective decay widths can be calculated using expression (8). The resulting values are listed in Table IV; their magnitudes were corrected for a small fraction of undetected protons lost in the background region.

Although one might have expected that $\Gamma^\downarrow(T_>)$ should be appreciably smaller than $\Gamma^\downarrow(T_<)$, due to the fact that the $T_>$ 2p-2h state density is smaller, it turns out that the spreading widths have about the same magnitude. However, the main result of this section is that the $T_>$ state predominantly decays by spreading, i.e.,

$$\frac{\Gamma^\downarrow(T_>)}{\Gamma(T_>)}=0.83\pm0.03$$

while the direct decay only represents a minor fraction

$$\frac{\Gamma^\uparrow(T_>)}{\Gamma(T_>)}=0.17\pm0.03 .$$

C. The statistical (γ,p) cross section

The cross section, shown in Fig. 7, for the reactions populating the densely spaced states above 4.5 MeV in ^{88}Sr was also derived in our ^{89}Y(γ,p) experiment.[17] Due to the complicated structure of these residual states, the decay mechanism for these processes has to be nondirect, and since preequilibrium decay is expected to be small in this energy region,[24] a statistical mechanism is most like-

TABLE IV. The respective decay widths of the $T_<$ and $T_>$ giant dipole resonances in ^{89}Y.

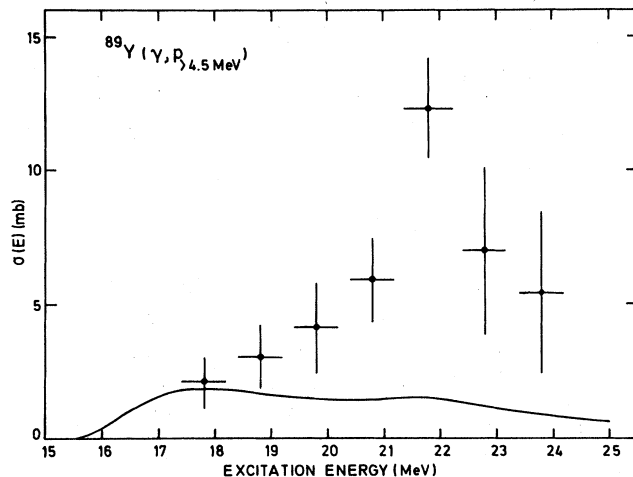| GDR	$\Gamma_p^\uparrow$ (MeV)	$\Gamma_n^\uparrow$ (MeV)	$\Gamma^\uparrow$ (MeV)	$\Gamma^\downarrow$ (MeV)	Γ (MeV)
$T_<$	0.35	0.80 (Ref. 23)	1.15	2.85	4.0
$T_>$	0.70	Negligible	0.70	3.30	4.0

FIG. 7. The data points show the experimental $^{89}Y(\gamma,p_{>4.5\,MeV})$ cross section for photoproton decay to states above 4.5 MeV in the residual nucleus ^{88}Sr. The full line represents the result of a Hauser-Feshbach calculation of the statistical (γ,p) part to this cross section, taking into account that only photoprotons with $T_p \geq 4$ MeV are detected. In the calculation it is assumed that both peaks in the total (γ,p) cross section have a $T_<$ character.

ly. As distinct from the direct decay cross sections (Figs. 5 and 6), it is evident that this statistical cross section reaches its maximum at the energy of the $T_>$ resonance, while on the other hand nearly no cross section is observed in the $T_<$ region. In order to demonstrate once more the $T_>$ nature of the second maximum in the total (γ,p) cross section, the statistical (γ,p) contribution to the cross section was calculated using a Hauser-Feshbach formalism, in the assumption that the two observed resonances have a $T_<$ character. The result, plotted in Fig. 7, is clearly inconsistent with the experimental data.

In Sec. III B it was concluded that the neutron decay of the $T_>$ state has a statistical origin. Due to the high separation energy ($=19.5$ MeV) for the isospin-allowed neutron channels, only a very small fraction of the $T_>$

(γ,n) cross section should be found in these channels. As a consequence, nearly the entire $T_>$ neutron decay must be caused by an isospin mixing mechanism and the following picture for the decay of the $T_>$ resonance emerges. In the course of time, most of the coherent 1p-1h $T_>$ strength is dampened into more and more complicated degrees of freedom dominated by isospin conservation. When the compound state level of complexity is reached, isospin symmetry breaking forces cause the decay of $T_>$ compound states into $T_<$ compound states. These latter states essentially generate the statistical neutron contribution to the $T_>$ channel, while the remaining part of the $T_>$ compound states almost exclusively decays in the photoproton channel in a statistical way.

IV. CONCLUSION

In the measured total $^{89}Y(\gamma,p)^{88}Sr$ reaction cross section, two distinct maxima are observed which have been identified as originating from the $T_<$ and $T_>$ coherent dipole states. Using existing (γ,n) results, the absolute $T_>$ strength could be derived and was found to be in good agreement with the estimate of Fallieros and Goulard.

Since the cross sections for various specific reaction channels were also determined, we were able to separate the direct decay from the statistical decay of the $T_>$ state in the proton channel. Again using (γ,n) data, both the escape $\Gamma^\uparrow$ and the spreading $\Gamma^\downarrow$ widths could be deduced. These results demonstrate the small direct decay probability $\Gamma^\uparrow/\Gamma = 0.17 \pm 0.03$ for the $T_>$ dipole state. As a final conclusion we observe that the $T_>$ strength detected in the photoneutron channel is almost entirely due to isospin mixing generated at the underlying compound state level of the $T_>$ resonance.

[1]P. Paul, in *Proceedings of the International Conference on Photonuclear Reactions and Applications, Asilomar, 1973*, edited by B. L. Berman (Lawrence Livermore Laboratory, University of California, 1973), p. 407.

[2]K. Shoda, Phys. Rep. **53**, 341 (1979).

[3]T. J. Bowles, R. J. Holt, H. E. Jackson, R. D. McKeown, A. M. Nathan, and J. R. Specht, Phys. Rev. Lett. **48**, 986 (1982).

[4]S. Fallieros and B. Goulard, Nucl. Phys. **A147**, 593 (1970).

[5]R. O. Akyüz and S. Fallieros, Phys. Rev. Lett. **27**, 1016 (1971).

[6]P. Paul, J. F. Amann, and K. A. Snover, Phys. Rev. Lett. **27**, 1013 (1971).

[7]J. D. Vergados and T. T. S. Kuo, Nucl. Phys. **A168**, 225 (1971).

[8]H. Arenhövel and J. M. Maison, Nucl. Phys. **A147**, 305 (1970).

[9]B. L. Berman, J. T. Caldwell, R. R. Harvey, M. A. Kelly, R. L. Bramblett, and S. C. Fultz, Phys. Rev. **162**, 1098 (1967).

[10]A. Leprêtre, H. Beil, R. Bergère, P. Carlos, A. Veyssière, and M. Sugawara, Nucl. Phys. **A175**, 609 (1971).

[11]K. Shoda, H. Miayse, M. Sugawara, T. Saito, S. Oikawa, A. Suzuki, and J. Uegaki, Nucl. Phys. **A239**, 397 (1975).

[12]M. Hasinoff, G. A. Fisher, H. M. Kuan, and S. S. Hanna, Phys. Lett. **30B**, 337 (1969).

[13]M. Hasinoff, G. A. Fisher, and S. S. Hanna, Nucl. Phys. **A216**, 221 (1973).

[14]W. M. Mason, G. Kernel, J. L. Black, and N. W. Tanner, Nucl. Phys. **A135**, 193 (1969).

[15]T. A. Hughes and S. Fallieros, Phys. Rev. C **3**, 1950 (1971).

[16]E. Van Camp, R. Van de Vyver, H. Ferdinande, E. Kerkhove, R. Carchon, and J. Devos, Phys. Rev. C **22**, 2396 (1980).

[17]E. Van Camp, R. Van de Vyver, E. Kerkhove, D. Ryckbosch, H. Ferdinande, P. Van Otten, and P. Berkvens, Phys. Rev. C **24**, 2499 (1981).

[18]R. Pitthan, F. R. Buskirk, E. B. Dally, J. O. Shannon, and W. H. Smith, Phys. Rev. C **16**, 970 (1977).

[19]R. L. Bunting and J. J. Kraushaar, Nucl. Data Sheets **18**, 87 (1976).

[20]T. A. Hughes, Phys. Rev. **181**, 1586 (1969).

[21]W. L. Wang and C. M. Shakin, Phys. Rev. C **5**, 1898 (1972).

[22]G. E. Brown, Nucl. Phys. **57**, 339 (1964).

[23]S. Cardman, Nucl. Phys. **A354**, 173c (1981).

[24]A. Agassi, H. A. Weidenmüller, and G. Mantzouranis, Phys. Rep. **22**, 145 (1975).